

# Photophysics and Photochemistry of a Lignin-like Quinoid Dimer, 4,4'-Dimethoxybiphenyl-2,5,2',5'-bisquinone, in Relation to Color Alteration of Woody Materials Exposed to Daylight

Stéphane Béarnais-Barbry,<sup>†,‡</sup> Roland Bonneau,<sup>\*,†</sup> and Alain Castellan<sup>‡</sup>

Laboratoire de Physico-Chimie Moléculaire and Laboratoire de Chimie des Substances Végétales, Université de Bordeaux I, 33405 Talence Cedex (France)

Received: July 22, 1999; In Final Form: October 6, 1999

4,4'-Dimethoxybiphenyl-2,5,2',5'-bisquinone **1** is thought to be issued, in wood and lignin-rich pulps, from the photochemical coupling and oxidation of methoxy(hydro)quinone. Under irradiation in solution, **1** is transformed to a highly colored dibenzofuran derivative, **2**, as unique photoproduct. The mechanism of the conversion **1** → **2** has been studied by laser flash photolysis and by quantum yield measurements in several solvents at various temperatures. The reaction proceeds via the triplet state of **1** and a cyclized **X** transient species which rearranges to **2** by a sequence of deprotonation–protonation reactions, quite efficiently in polar or acidified solutions but with a low yield in nonpolar solvents. As temperature increases, the quantum yield increases in polar solutions but decreases in nonpolar solvents. This unusual temperature dependence is explained by activation energy barriers on the cyclization  $^3\mathbf{1}^* \rightarrow \mathbf{X}$  and reopening  $\mathbf{X} \rightarrow \mathbf{1}$  elementary reactions,  $\approx 35.5$  and  $58.5$  kJ/mol respectively, and by a conversion  $\mathbf{X} \rightarrow \mathbf{2}$  much faster in polar solvents than in nonpolar ones. The zwitterionic or biradicaloid structure of **X** is discussed on the basis of semiempirical calculations (AM1 or PM3) and of spectroscopic and kinetic measurements. Under laser flash photolysis conditions, a special mechanism involving a second-order rearrangement of **X** was found to be very efficient in any type of solvents.

## Introduction

The major components of wood and mechanical pulps are cellulose, hemicelluloses, and lignin. Of these, only lignin is considered to contribute in a major way to wood and pulp color.<sup>1</sup> Other possible contributors to color are substances called extractives which are minor wood components. Lignocellulosic materials such as wood<sup>2</sup> and mechanical pulps<sup>3</sup> are very sensitive toward exposure to sunlight where strong yellowing is observed. Recently major advances in mechanical pulping and bleaching have provided the means of manufacturing bleached high-yield (> 90%) pulps with a high brightness (> 80% ISO).<sup>4</sup> Such pulps could potentially replace bleached kraft pulps for high-value paper products. The mechanisms of color alteration of woody materials were approached using model compounds<sup>5</sup> or studying ground wood pulps<sup>6</sup> and wood.<sup>7,8</sup> These studies have shown the importance of *o*-quinoid lignin structures which are formed under light irradiation. Also, *p*-quinones and hydroquinones such as 3-methoxy-5-substituted *p*-benzoquinones and 3-methoxy-5-substituted *p*-hydroquinones were involved in the color reversion of bleached mechanical pulps.<sup>9,10</sup> These structures are formed by the Dakin reaction from the corresponding substituted *p*-carbonyl phenols when the pulps are bleached with hydrogen peroxide in an alkaline medium. The photochemical reactivity of 2-methoxy-hydroquinone **3** and 2-methoxy-*p*-quinone **4** in aerated dimethoxyethane solution was investigated by Forsskåhl et al.<sup>11</sup> It was observed that irradiation of compound **3** gives the quinone **4** and the dimer **5**, while irradiation of the quinone **4** or dimer **5** (see Scheme 1) generates the 8-hydroxy-3,7-dimethoxydibenzofuran-1,4-quinone **2** probably via the 4,4'-

dimethoxybiphenyl-2,5,2',5'-bisquinone **1**. Compound **1** is easily converted by irradiation to the highly colored dibenzofuran **2**.<sup>11,12</sup> The reactions involving the methoxy-*p*-quinone, the dimer quinones, and their rearranged photoproducts might play a significant role in the production of color in woody materials.

The photoconversion of the bisquinone **1** in the dibenzofuran **2** resembles the reaction of photocyclization of many substituted *p*-benzoquinones such as 2,6-diphenyl-*p*-benzoquinone,<sup>13</sup> isopropenyl-*p*-benzoquinone,<sup>14</sup> and dimethylamino-*p*-benzoquinone.<sup>15</sup> It was shown, by laser flash photolysis, that the photocyclization of the phenyl- and 4-anisyl-*p*-benzoquinones in dibenzofuran<sup>16,17</sup> involves the triplet state of the quinone and an hypothetical cyclized transient species, **X**, which, depending on the solvent, rearranges to the photoproduct or reverts to the starting quinone. However, this mechanism is certainly not valid for all of the substituted *p*-benzoquinones yielding a benzofuran moiety upon photocyclization. This article describes photochemical and photochemical analyses of the formation of compound **2** using continuous and flash photolysis. The observation of the intermediate **X** allowed us a complete kinetic analysis of the different photochemical pathways leading from the bisquinone **1** to the dibenzofuran **2**.

## Experimental Section

**Solvents and Products.** 4,4'-Dimethoxybiphenyl-2,5,2',5'-bis-*p*-benzoquinone, **1**, was prepared from vanillin (Aldrich) according to the method described by Erdtman,<sup>18</sup> involving the "quinhydrol" intermediate **5**. Yellow crystals were obtained by recrystallization of the crude product in acetic anhydride under nitrogen and were identified as **1** by <sup>1</sup>HNMR spectroscopy (Bruker AC250, 250 MHz, CDCl<sub>3</sub>):  $\delta$  6.77 (s, 2H), 6.04 (s, 2H), 3.87 (s, 6H); mp 216 °C (ref 18, 212–214 °C). UV:  $\lambda_{\max}$   $\approx 366$  nm,  $\epsilon = 1500 \pm 50$  M<sup>-1</sup>cm<sup>-1</sup> in a variety of solvents.

\* Corresponding author. E-mail: bonneau@cribx1.u-bordeaux.fr; a.castellan@ipin.u-bordeaux.fr.

<sup>†</sup> Laboratoire de Physico-Chimie Moléculaire.

<sup>‡</sup> Laboratoire de Chimie des Substances Végétales.

## SCHEME 1: Structures of Compounds 1–5

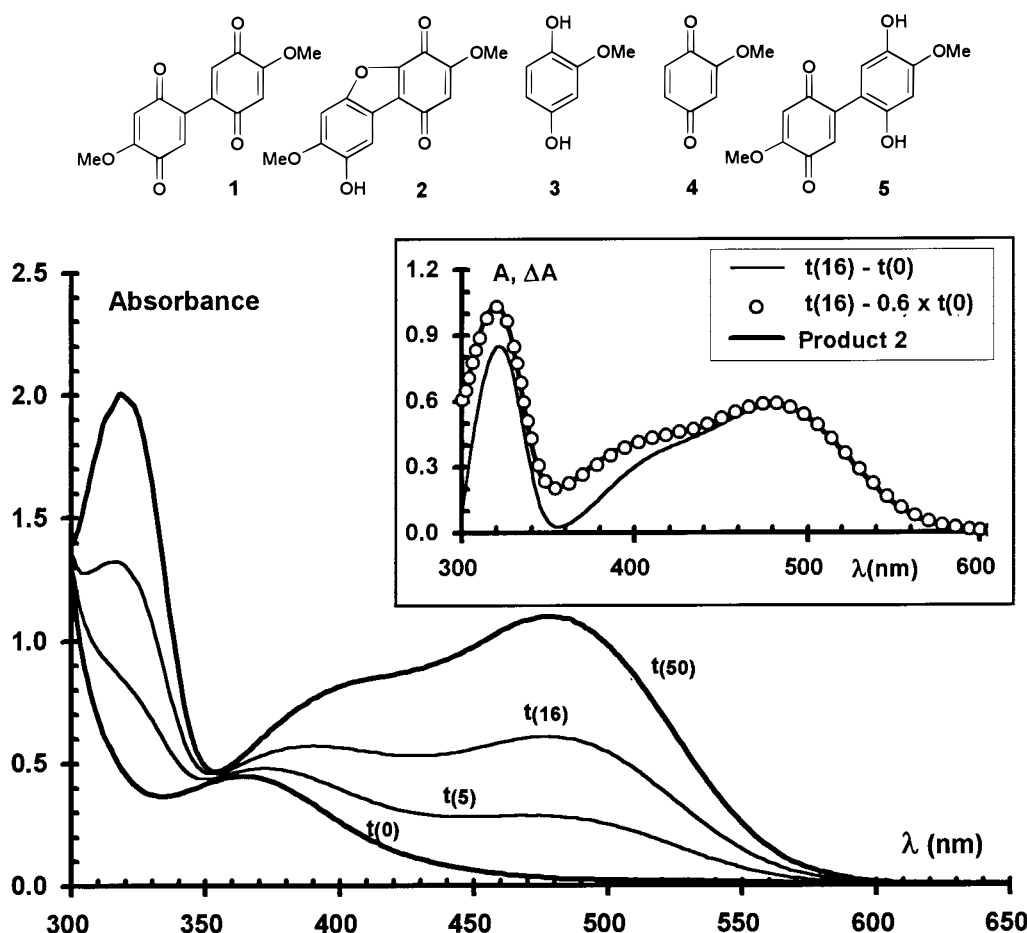


**Figure 1.** Absorption spectrum of **1** ( $\approx 0.7$  mM) in  $N_2$ -flushed acetonitrile before and after irradiation at 355 nm during 5, 16, and 50 min. Inset: (—), simple differential spectrum  $t_{(16)} - t_{(0)}$ ; (○), the same differential spectrum when assuming that 40% of **1** has been transformed, i.e.,  $t_{(16)} - 0.6 \times t_{(0)}$ ; (— through circles), absorption spectrum of an authentic sample of **2**.

8-Hydroxy-3,7-dimethoxydibenzofuran-1,4-quinone, **2**, was prepared by irradiation of **1** in anhydrous methanol with two 400 W Hg lamps, according to the method described by Shand and Thomson.<sup>19</sup> Red needle crystals were obtained after recrystallization in ethanol and were identified as **2** by <sup>1</sup>HNMR spectroscopy (250 MHz,  $CD_3COCD_3$ ):  $\delta$  7.38 (s, 1H), 7.31 (s, 1H), 5.91 (s, 1H), 3.97 (s, 3H), 3.88 (s, 3H); mp 245 °C (ref 19, 248–249 °C). UV:  $\lambda_{max}$  [ $\epsilon$ ] = 466 nm [4500  $M^{-1}cm^{-1}$ ] in benzene, 478 nm [4620] in MeCN, 498 nm [4750] in EtOH.

Acetonitrile (Prolabo), benzene (Carlo Erba), benzonitrile (Aldrich), and dichloromethane (SDS) were of spectroscopic grade. Ethanol (95%, for UV spectroscopy) was purchased from Prolabo. Acetic acid and anisole were purchased from Rhône-Poulenc, and di-*n*-butyl ether from Aldrich. These solvents were used without further purification, but acetonitrile and benzene were stored on 4 Å molecular sieves.

**Continuous Irradiation.** Continuous irradiation was performed by using a 2 kW Xenon arc coupled to an irradiation monochromator (Jobin-Yvon) providing about  $3 \times 10^{15}$  photons  $cm^{-2} s^{-1}$  on a 5 nm spectral bandwidth around 355 nm. Spectra of irradiated solutions were recorded on an HP8452A diode array spectrophotometer.

**Laser Flash Photolysis (LFP).** The laser flash photolysis apparatus used a crossed-beam arrangement. The sample in a  $10 \times 10$  mm cell was excited by single 355 nm pulses (5–30 mJ, 200 ps) provided by a frequency-tripled mode locked Nd:YAG laser (Quintel). The detection system, with a 5-ns response time, consisted of a pulsed Xenon arc, a prism monochromator,

a red sensitive photomultiplier (Hamamatsu R-446), and a Tektronix TDS 620B digital oscilloscope connected to a microcomputer.

## Results

**Continuous Irradiation.** Under photolysis at  $355 \pm 5$  nm of a solution of **1** in  $N_2$ -flushed acetonitrile ( $[1] \approx 0.7$  mM), a new absorption develops from 580 to 300 nm (lower limit of the domain where absorbance measurements are significant) and rapidly overcomes the absorption of **1**. The absorption spectrum of the species responsible for this absorption is obtained as the difference between the absorption spectrum recorded after a short irradiation and one recorded before irradiation (multiplied by a factor corresponding to the percentage of non photolyzed **1**). The resulting spectrum exactly fits the absorption spectrum of an authentic sample of **2** in the same solvent, characterized by maxima at 320 and 478 nm and a minimum at 354 nm as shown in Figure 1. Thin-layer chromatography (Silica gel;  $CH_2Cl_2:Et_2O$ , 90:10) of the reaction mixture after a prolonged irradiation (more than 50% of **1** photolyzed) revealed the presence of only two products, **1** and **2**. This indicates that the chemical yield of the photoconversion  $1 \rightarrow 2$  is (close to) unity and that **2**, which absorbs at the excitation wavelength, is photostable. The latter point was checked by irradiation of a solution of **2** during a period of time five times longer than the longest irradiation performed during this study: no measurable decrease of the absorbance at 478 nm could be detected.

**TABLE 1: Quantum Yield of Formation of 2 ( $\Phi_{12}$ ) at 27 °C, in Various N<sub>2</sub>-Flushed Solvents Characterized by Their  $E_T(30)$  Polarity Parameter**

solvent	$\Phi_{12}$	$E_T(30)$
PhH	0.08 ± 0.01	34.5
PhOMe	0.18 ± 0.02	37.2
CH <sub>2</sub> Cl <sub>2</sub>	0.45 ± 0.02	41.1
PhCN	0.45 ± 0.02	42.0
MeCN	0.48 ± 0.02	46.0
EtOH	0.53 ± 0.05	51.9

**TABLE 2: Quantum Yield of Formation of 2 in N<sub>2</sub>-Flushed Benzene (PhH) Containing Various Amounts of Acetic Acid (AcOH) or Ethanol (EtOH)**

[AcOH] or [EtOH] (mM)	$\Phi_{12}$ in PhH + AcOH <sup>a</sup>	$\Phi_{12}$ in PhH + EtOH <sup>b</sup>
0	0.09	0.125
0.1	0.17	
0.2	0.24	
0.5	0.37	
1.0	0.48	
5.0	0.52	0.39
10	0.48	0.40

<sup>a</sup> At 26 °C. <sup>b</sup> At 18 °C.

The quantum yield of the photoconversion **1** → **2** was determined by measuring (i) the rate of growth of the absorbance at 478 nm,  $d(A_{478})/dt$ , easily converted to the rate of growth of the concentration of **2** since the absorption coefficient of **2** at 478 nm is known and (ii) the flux of photons irradiating the sample, obtained by actinometry using the photocoloration of Aberchrome 540.<sup>20</sup> The number of photons absorbed by the sample during a short period of time was then calculated from the value of the absorbance of **1** at 354 nm. As the reaction progresses, the absorbance of **1** decreases and an increasing fraction of the excitation is absorbed by **2** so that the curve  $A_{478}$  vs time curves downward. The values of  $d(A_{478})/dt$  were thus determined from the initial slope of the curve  $A_{478}$  vs time, accurately determined by repeatedly recording the spectra after short irradiations (10 to 20 s) corresponding to photolysis of only a few percents of **1**. The plot of  $A_{478}$  vs time is then nicely linear and its slope is easily determined. On prolonged irradiation, up to conversion of 10 to 30% of **1**, the curvature of the plot  $A_{478}$  vs time was evident and the resulting curve was fitted by non linear regression to a function  $A = at + bt^2$  where the  $a$  coefficient is the initial slope of the curve. This method was used as an alternative to the previous one, especially in solvents such as benzene where the ratio  $\epsilon_{354}^{(2)}/\epsilon_{354}^{(1)}$  is much larger than in acetonitrile so that the screening effect of **2** is more important.

In N<sub>2</sub>-flushed solutions, the quantum yield of formation of **2** in acetonitrile at 27 °C was found to be 0.48 ± 0.02. The values determined in other solvents using the same procedure are listed in Table 1: the quantum yield is small in benzene and increases as the polarity of the solvent, quantified by the value of its  $E_T(30)$ ,<sup>21</sup> the polarity parameter defined by Reichardt,<sup>22</sup> increases.

The value of  $\Phi_{12}$  in benzene increases rapidly upon addition of small amounts of acetic acid or ethanol. As shown in Table 2, concentrations of these compounds as low as 10<sup>-2</sup> M boost the value of  $\Phi_{12}$  up to a limit in the range 0.4–0.5, i.e., comparable to the value obtained in polar solvents. Therefore, the value of  $\Phi_{12}$  in benzene could be due, at least in part, to the presence of trace amounts of moisture in the solvent (although benzene was stored over molecular sieves).

It seems reasonable to assume that the reaction proceeds via the triplet state of **1**. This hypothesis was checked by measuring the influence of dissolved oxygen on the quantum yield in solutions flushed with air N<sub>2</sub>, O<sub>2</sub>, and a 1:1 mixture of N<sub>2</sub> and O<sub>2</sub>. The results are given in Table 3 where the last line gives

**TABLE 3: Quantum Yield of Formation of 2 in Solvents Flushed with a Gas Mixture Containing Various Amounts of O<sub>2</sub> (measurements at 27 °C)**

O <sub>2</sub> content in flushing gas	$\Phi_{12}$ in EtOH	$\Phi_{12}$ in MeCN
0% O <sub>2</sub>	0.55	0.48
21% O <sub>2</sub>	0.18	0.16
50% O <sub>2</sub>	0.08	0.08
100% O <sub>2</sub>	0.03	0.04
$k_q\tau$ (M <sup>-1</sup> )	1200	1100

**TABLE 4: Effect of Temperature on the Quantum Yield of Formation of 2**

$T$ (°C)	$\Phi_{12}$ (meas)	$\Phi_{TX}^a$	$\Phi_{X2}^a$
	in benzene <sup>b</sup>		
11	0.14	0.430	0.325
20	0.12	0.543	0.221
27	0.08	0.624	0.129
35	0.05	0.705	0.071
	in MeCN <sup>c</sup>		
12	0.303	0.291	1.04
27	0.42	0.466	0.92
38	0.60	0.592	1.01

<sup>a</sup> See Discussion and Interpretation section for definition of these yields. <sup>b</sup>  $\Phi_{TX}$  calculated with  $k_0 = 0.73 \times 10^6 \text{ s}^{-1}$ ,  $\Delta E = 35.1 \text{ kJ/mol}$  and  $A = 10^{12.16} \text{ s}^{-1}$ . <sup>c</sup>  $\Phi_{TX}$  calculated with  $k_0 = 1.08 \times 10^6 \text{ s}^{-1}$ ,  $\Delta E = 36 \text{ kJ/mol}$  and  $A = 10^{12.2} \text{ s}^{-1}$ .

the value of “ $k_q\tau$ ” obtained by assuming that only one intermediate species, **31\***, with a lifetime  $\tau$  is quenched with a rate constant  $k_q$ .<sup>23</sup> If this assumption is correct and with a value of  $k_q$  around  $3 \times 10^9 \text{ M}^{-1} \text{ s}^{-1}$  as it is usually for the quenching of triplet states by O<sub>2</sub>, the lifetime of **31\*** would be 400 ns in both solvents. This indicates a  $\pi\pi^*$  nature for **31\***: the lifetime of a  $n\pi^*$  triplet would be much shorter in EtOH than in MeCN due to H-abstraction, and this would give reduction product(s) which are not detected.

The influence of the temperature on the reaction quantum yield gave puzzling results presented in Table 4: as the temperature increases,  $\Phi_{12}$  increases in acetonitrile but it decreases in benzene!

**Laser Flash Photolysis. Spectral Data.** A series of traces “optical transmission vs time” recorded every 10 or 20 nm between 330 and 830 nm have been converted into absorption spectra at given times after excitation as shown in Figure 2 for a N<sub>2</sub>-flushed solution in MeCN.

Immediately (5–10 ns) after excitation, a first transient species absorbs over the entire visible region. It is characterized by an absorption band with a maximum at 450 nm, a minimum at 390 nm, and a second band rapidly growing from 360 to 330 nm. This transient species decays with a lifetime around 500 ns, and gives rise to a second transient species, **X**, characterized by two absorption bands with maxima at 370 and around 750 nm, which decays during a few tens of microseconds. After 100  $\mu\text{s}$ , the **X** species has disappeared and a new absorption spectrum is obtained with a maximum at 480 nm, a minimum at 360 nm, and a shape that is nearly identical to the differential absorption spectrum shown in the inset of Figure 1. It corresponds to stable products: the major one is easily identified as the final product **2** and the minor one is responsible for the larger value of the absorbance in the 350–380 nm range.

In N<sub>2</sub>-flushed benzene and benzonitrile, the spectral features of the transient absorptions are nearly the same as in acetonitrile. In benzene, the following slight differences can be noticed: (i) a broadening, especially on the red side, of the absorption band of the first species with a maximum around 450 nm; (ii) a shift of the maximum of the red band of the **X** species from 750 to 800 nm and a slight increase of the ratio between the intensities of the UV (370 nm) and red (800 nm) bands.

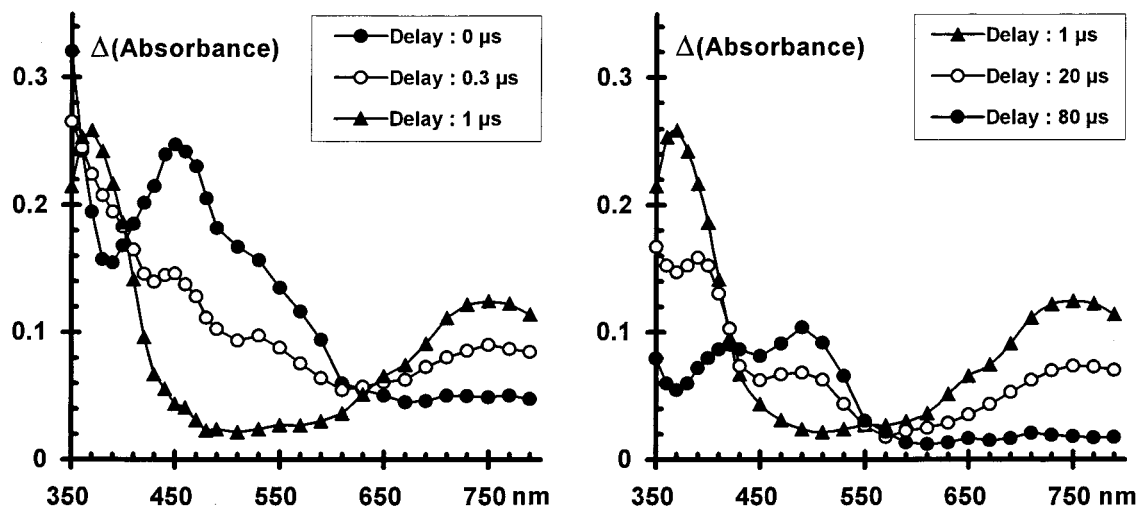


Figure 2. Transient absorption spectra in acetonitrile in the time ranges 0.005–1  $\mu$ s and 1–80  $\mu$ s.

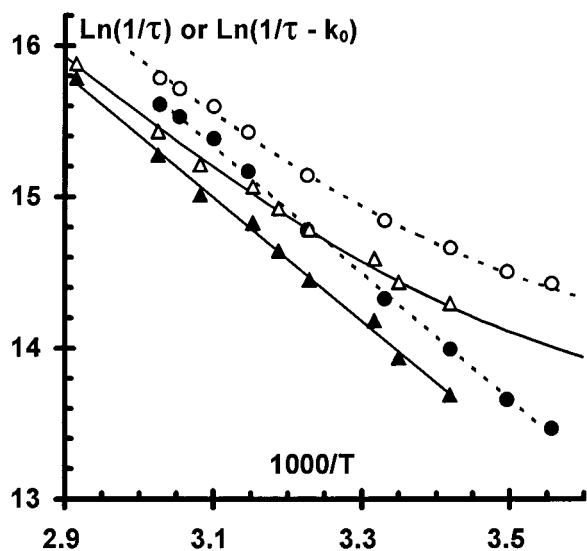


Figure 3. Arrhenius plots for the triplet lifetime in benzene ( $\Delta$ ) and acetonitrile (O). Open symbols:  $\text{Ln}(1/\tau)$ . Filled symbols:  $\text{Ln}(1/\tau - k_0)$  with  $k_0 = 0.73$  and  $1.14 \times 10^6 \text{ s}^{-1}$ , respectively.

Surprisingly, the amplitude of the final increase of the absorbance in the 350–550 nm region, assigned to **2**, is nearly the same as in acetonitrile, whereas, under continuous irradiation, the quantum yield of formation of **2** in benzene is 6 times smaller than in acetonitrile.

**Kinetic Data.** The first transient species is formed within the time resolution of our LFP setup ( $\approx 5$  ns) and it decays according to a first-order law with a lifetime,  $\tau$ , which depends slightly on the solvent and strongly on the temperature. This lifetime depends also on the concentration of  $\text{O}_2$  dissolved in the solution, and the following values of the quenching rate constant  $k_q$  were obtained from the linear plots of  $1/\tau$  vs  $[\text{O}_2]$ :  $k_q = 1.6 \times 10^9$  and  $2.5 \times 10^9 \text{ M}^{-1}\text{s}^{-1}$  in benzene and acetonitrile, respectively. These values, approximately equal to 1/9 of the diffusion rate constant in these solvents, are typical for the quenching of a triplet state by  $\text{O}_2$  and support the idea that the first species must be identified as the triplet state of **1**.

The temperature dependence of the lifetime of this first transient species was studied in benzene and acetonitrile on the range 8–70  $^\circ\text{C}$ , and the corresponding Arrhenius plots,  $\text{Ln}(1/\tau)$  vs  $1/T$  are given in Figure 3. These plots are clearly curved indicating that two processes, at least, contribute to the decay of the observed species: one with a low (or null) activation

TABLE 5: Kinetics Parameters for the Decay of the Triplet State of **1**

solvent	benzene	acetonitrile
$k_0$ ( $10^6 \text{ s}^{-1}$ )	$0.73 \pm 0.18$	$1.14 \pm 0.17$
$\log(A_1)$	$12.16 \pm 0.40$	$12.20 \pm 0.30$
$\Delta E_1$ (kJ/mol)	$35.1 \pm 2.5$	$36 \pm 1.7$

energy and a rate constant  $k_0$ , another with a rate constant  $k_1 = A_1 \exp(-\Delta E_1/RT)$ . Nonlinear curve fitting of  $1/\tau = k_0 + A_1 \exp(-\Delta E_1/RT)$  vs  $1/T$  gave the values of  $k_0$ ,  $A_1$ , and  $\Delta E_1$  listed in Table 5.

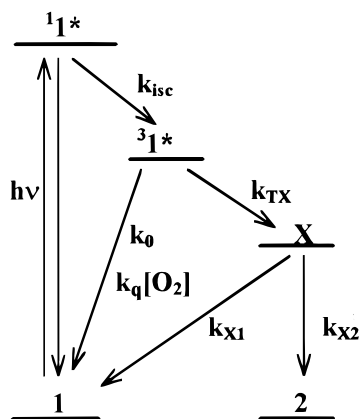
Since the quantum yield of the reaction in benzene is very sensitive to the addition of trace amounts of acetic acid or alcohol, we have checked the effect of these compounds on the lifetime of the first species. No significant effect could be observed up to  $[\text{AcOH}] > 0.5 \text{ M}$  whereas the quantum yield of the reaction reaches a limit values when  $[\text{AcOH}] > 2 \text{ mM}$ .

The decay of the second species, **X**, is not first order. In acetonitrile and monitored at 750 nm, it can be analyzed as the sum of first and second-order processes, with  $k_2/\epsilon \approx 5 \times 10^5 \text{ cm s}^{-1}$  and a first-order rate constant  $k_1 \approx 2 \times 10^4 \text{ s}^{-1}$ . In benzene, it can be analyzed as a “good” second-order reaction with  $k_2/\epsilon = 1.9 \times 10^6 \text{ cm s}^{-1}$  at 800 nm and a possible contribution of a first-order process would correspond to  $k_1 \approx 10^4 \text{ s}^{-1}$ . A second-order analysis at 370 nm yielded  $k_2/\epsilon \approx 10^6 \text{ cm s}^{-1}$ , about half of the value measured at 800 nm, in agreement with the ratio of the  $\epsilon$  values at these two wavelengths. The first value is more accurate than the second one because the results of the analysis at 370 nm greatly depend on the estimation of the value of the residual permanent absorption, whereas, at 800 nm, this value is zero.

Upon addition of acetic acid in benzene, the kinetics of the decay of the **X** species progressively changes from a second-order to a first-order process. The values of  $k_1$  and  $k_2/\epsilon$  obtained for solutions containing various amounts of acetic acid in benzene and acetonitrile are given in Table 6. The increase of  $k_1$  as a function of  $[\text{AcOH}]$  indicates that the **X** species reacts with (or is quenched by) acetic acid. The slope of the linear plots of  $k_1$  vs  $[\text{AcOH}]$  gives the values of the rate constant for this process,  $k_{\text{Ac}} = 1.49 \times 10^7 \text{ M}^{-1} \text{ s}^{-1}$  in benzene and  $4.3 \times 10^5 \text{ M}^{-1} \text{ s}^{-1}$  in acetonitrile, and the intercept gives the rate constant associated to the first-order component of the decay of **X** as equal to  $1.38 \times 10^4 \text{ s}^{-1}$  in benzene. This value seems more reliable than the estimate obtained from the analysis of decays in the absence of AcOH where the second-order

**TABLE 6: Rate Constants of First- and Second-Order Decay Processes of the X Species in the Presence of Various Amounts of Acetic Acid**

[AcOH] (mM)	$k_1$ ( $10^4$ s $^{-1}$ )	$k_2/\epsilon$ ( $10^6$ cm s $^{-1}$ )
added	in benzene	( $\epsilon$ at 800 nm)
0	1	1.9
1	3.4	1.7
10	16	1.6
20	31.5	1.6
added	in MeCN	( $\epsilon$ at 760 nm)
0	2.0	0.44
10	2.4	0.57
20	2.8	0.54
50	3.8	0.57
100	6.5	0.46

**SCHEME 2: Simplified Reaction Mechanism**

component was largely predominant. A more accurate value ( $7.7 \times 10^3$  s $^{-1}$ ) will be obtained later by an independent method.

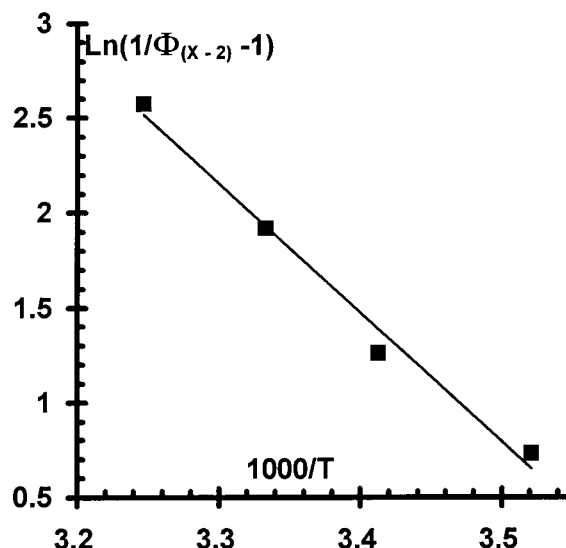
**Discussion and Interpretation**

**Proposed Mechanism.** The above results may be rationalized by the mechanism represented in Scheme 2. The first step is intersystem crossing of the excited singlet state  $^1\mathbf{1}^*$  to the triplet  $^3\mathbf{1}^*$ , a  $\pi\pi^*$  state, with a yield probably close to unity (the fluorescence from  $^1\mathbf{1}^*$  is extremely weak and its quantum yield is  $< 0.1\%$ ).

The next step is the cyclization of  $^3\mathbf{1}^*$  into an intermediate  $\mathbf{X}$ . Its efficiency,  $\Phi_{\text{TX}}$ , is determined by the competition between deactivation of  $^3\mathbf{1}^*$  to the  $\mathbf{1}$  ground state and cyclization to  $\mathbf{X}$ . The two components identified during the study of the triplet lifetime as a function of temperature obviously correspond to these two processes: (i) the deactivation of  $^3\mathbf{1}^*$  to  $\mathbf{1}$ , associated to  $k_0 \approx 10^6$  s $^{-1}$  with a null activation energy and (ii) the cyclization to  $\mathbf{X}$ , with an activation energy  $35.5 \pm 2$  kJ/mol and a frequency factor  $A \approx 10^{12 \pm 0.5}$  s $^{-1}$ . The order of magnitude of the  $A$  factor indicates a spin-allowed intramolecular process so that, most certainly,  $\mathbf{X}$  is first produced as a triplet biradical which may rapidly equilibrate with (or be transformed into) a singlet biradical and/or a zwitterionic structure.

The values of the yield of cyclization,  $\Phi_{\text{TX}} = k_{\text{TX}}/(k_0 + k_{\text{TX}})$  with  $k_{\text{TX}} = A \exp(-\Delta E/RT)$ , calculated with the values of  $k_0$ ,  $A$  and  $\Delta E$  given in Table 5, are shown in Table 4. In acetonitrile, the values of  $\Phi_{\text{TX}}$  compare quite well with those of the overall reaction quantum yield,  $\Phi_{12}$ , whereas the situation is completely different in benzene.

The value of  $\Phi_{\text{TX}}$  also depends on  $\text{O}_2$  since  $\Phi_{\text{TX}} = k_{\text{TX}}/(k_0 + k_{\text{TX}} + k_{\text{q}}[\text{O}_2])$ . The effects of oxygen on  $\Phi_{\text{TX}}$  and on the overall reaction are roughly the same: in acetonitrile, the  $k_{\text{q}}\tau$  product obtained from the values of  $k_{\text{q}}$  and  $\tau$  measured by LFP for the triplet ( $k_{\text{q}}\tau = 1000$ ) is close to the value of the “global

**Figure 4.** Arrhenius plot for the reopening reaction of  $\mathbf{X}$  in benzene.

$k_{\text{q}}\tau$ , 1100, obtained from the plot of  $\Phi_{12}^\circ/\Phi_{12}$  vs  $[\text{O}_2]$ . This supports the hypothesis that oxygen interacts only with  $^3\mathbf{1}^*$  and/or does not change the yield of the next step(s). The effect of  $\text{O}_2$  seems to be relatively independent of the solvent since similar values of the  $k_{\text{q}}\tau$  product were obtained in ethanol ( $1200$  M $^{-1}$ ) and in benzene ( $800$  M $^{-1}$ ).

The last step of the mechanism is the conversion of  $\mathbf{X}$  into  $\mathbf{2}$  by a sequence of deprotonation–protonation reactions resulting, formally, in a 1,6-migration of an H atom from the cyclization center to the oxygen in para position of the furan moiety.

The comparison of the values of  $\Phi_{\text{TX}}$  with those of  $\Phi_{12}$ , in Table 4, indicates that for the conversion of  $\mathbf{X} \rightarrow \mathbf{2}$ ,  $\Phi_{\text{X2}}$  is quantitative or close to unity in acetonitrile whereas, in benzene, this yield decreases from 0.32 to 0.07, as the temperature increases from 11 to 35 °C. This implies that, in benzene, a strongly temperature-dependent process competes with the conversion  $\mathbf{X} \rightarrow \mathbf{2}$ . This is most probably a reopening of  $\mathbf{X}$  into  $\mathbf{1}$  since no product other than  $\mathbf{1}$  and  $\mathbf{2}$  could be detected after continuous irradiation. With this assumption, the yield of the conversion  $\mathbf{X} \rightarrow \mathbf{2}$  is  $\Phi_{\text{X2}} = k_{\text{X2}}/(k_{\text{X1}} + k_{\text{X2}})$  where  $k_{\text{X1}}$  and  $k_{\text{X2}}$ , the rate constants of the reactions  $\mathbf{X} \rightarrow \mathbf{1}$  and  $\mathbf{X} \rightarrow \mathbf{2}$ , can be written as  $k_{\text{Xn}} = A_{\text{Xn}} \times \exp(-\Delta E_{\text{Xn}}/RT)$ . From these relations, simple mathematics give

$$\text{Ln}[(1/\Phi_{\text{X2}}) - 1] = \text{Ln}[(\Phi_{\text{TX}}/\Phi_{12}) - 1] = \text{Ln}(A_{\text{X1}}/A_{\text{X2}}) + (\Delta E_{\text{X2}} - \Delta E_{\text{X1}})/RT$$

The plot of  $\text{Ln}[(\Phi_{\text{TX}}/\Phi_{12}) - 1]$  vs  $1/T$ , in Figure 4, gives estimates<sup>24</sup> of  $A_{\text{X1}}/A_{\text{X2}}$  and  $\Delta E_{\text{X2}} - \Delta E_{\text{X1}}$  to be  $A_{\text{X1}}/A_{\text{X2}} = 4.8 \times 10^{10}$  and  $\Delta E_{\text{X1}} - \Delta E_{\text{X2}} = 56.8$  kJ/mol.

Assuming that  $\Delta E_{\text{X2}}$  is small and may be set to zero,<sup>25</sup>  $A_{\text{X2}} \approx k_{\text{X2}}$  and  $\Delta E_{\text{X1}} \approx 56.8$  kJ/mol. It was shown above, from the kinetic analysis of the complex decay of the absorption of  $\mathbf{X}$  in benzene (with or without added AcOH), that  $(k_{\text{X1}} + k_{\text{X2}}) \approx 1.4 \times 10^4$  s $^{-1}$ . From this value and with  $\Phi_{\text{X2}} = k_{\text{X2}}/(k_{\text{X1}} + k_{\text{X2}}) = \Phi_{12}/\Phi_{\text{TX}} = 0.129$  at 27 °C, one gets  $k_{\text{X2}} \approx 1.8 \times 10^3$  s $^{-1}$ ,  $k_{\text{X1}} \approx 1.2 \times 10^4$  s $^{-1}$ , and thus  $A_{\text{X1}} \approx 8.6 \times 10^{13}$  s $^{-1}$ .

The values of  $k_{\text{X1}}$  and  $k_{\text{X2}}$  may be evaluated by another way. The addition of 0.1 mM AcOH in benzene increases the value of  $\Phi_{12}$  from 0.08 to 0.17 (see Table 2) but has strictly no effect on the triplet and therefore on  $\Phi_{\text{TX}}$ . Acetic acid clearly increases the value of  $\Phi_{\text{X2}}$  by opening new channel to the conversion  $\mathbf{X} \rightarrow \mathbf{2}$ . The rate constant of this reaction of  $\mathbf{X}$  with AcOH, obtained from the slope of the linear plot of the data given in

## SCHEME 3: Possible Limit Structures for the X and X' Species

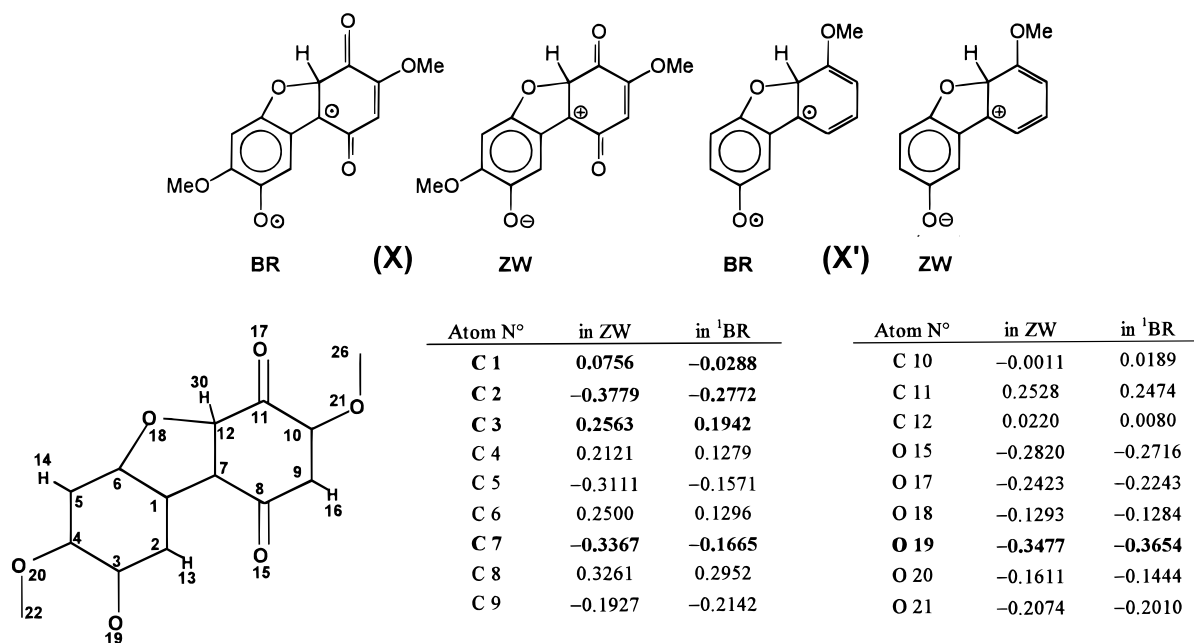


Figure 5. Charges calculated for the singlet biradical and the zwitterionic structures of the X intermediate, using the AM1 module of AMPAC 6.01

Table 6, is  $k_{Ac} = 1.5 \times 10^7 \text{ M}^{-1} \text{ s}^{-1}$ . Then, the values of  $\Phi_{X2} = (k_{X2} + k_{Ac} [\text{AcOH}]) / (k_{X1} + k_{X2} + k_{Ac} [\text{AcOH}])$ , obtained from the ratio  $\Phi_{12} / \Phi_{TX}$  as equal to 0.129 and 0.274 when  $[\text{AcOH}] = 0$  and 0.1 mM respectively, give  $k_{X1} = 6.7 \times 10^3 \text{ s}^{-1}$ ,  $k_{X2} = 10^3 \text{ s}^{-1}$ , and  $A_{X1} = 4.8 \times 10^{13} \text{ s}^{-1}$ . Thus, the two methods give similar values for  $A_{X1}$ , in the range  $(4.8-8.6) \times 10^{13} \text{ s}^{-1}$ , quite reasonable for the frequency factor of an intramolecular reaction favored by entropy (the rotation around the 1-1' C-C bond is restored by reopening).

The reopening reaction exists in acetonitrile too, with  $A$  and  $\Delta E$  factors probably similar to those estimated in benzene. However, with  $A_{X1} \approx 5 \times 10^{13} \text{ s}^{-1}$  and  $\Delta E_{X1} \approx 58.5 \text{ kJ/mol}$ ,  $k_{X1} \approx 3.5 \times 10^3 \text{ s}^{-1}$  at room temperature, a relatively small value compared to the rate constant of the first-order component of the decay of X in acetonitrile,  $k_1 \approx 2 \times 10^4 \text{ s}^{-1}$ . Therefore  $k_{X2} \gg k_{X1}$  and the value of  $\Phi_{X2}$  is close to unity in acetonitrile.

In the absence of acid, the reaction is much more efficient in polar solvents than in benzene because the rate of the conversion  $X \rightarrow 2$  increases as the solvent polarity increases. This suggests a mechanism in which the cyclization center, C(12), loses a proton to give the deprotonated form of the final product, 2<sup>-</sup>; see atom numbering on Figure 5. This process restores the quinone moiety and is energetically favorable when the solvent is polar enough to ensure the solvation of the resulting ions, 2<sup>-</sup> and H<sup>+</sup>. These ions then recombine to give the final product with the H atom being transferred from C(12) to O(19) by this sequence of deprotonation-protonation reactions. This mechanism seems somewhat different from the one observed in the photocyclization of *m*-anisylbenzoquinone, AnBQ,<sup>26</sup> where X', the species equivalent to X (see Scheme 3), must be first protonated on the O atom equivalent to O(19) and the resulting cation then expels as a proton the H atom located on the carbon atom equivalent to C(12). This alternative mechanism may also occur in the case of X since the addition of acetic acid in benzene is much more efficient than in ethanol to boost the yield of the reaction (see Table 2). However, that the difference between the rate constants of the reaction of X and X' with AcOH respectively equal to  $1.5 \times 10^7 \text{ M}^{-1} \text{ s}^{-1}$  and  $4.6 \times 10^9 \text{ M}^{-1} \text{ s}^{-1}$  in benzene, suggests that structures of these species,

TABLE 7: Calculated Differences between the Enthalpies of Formation of Various Structures of X (or X') and 2 (or 2') and Those of the Parent Compound, 1 (or AnBQ)

$\Delta H_{(p)} - \Delta H_{(1)}$ (kJ/mol)	bis-quinone 1 system	AnBQ system
X (ZW)	115.8 <sup>a</sup> ; 97 <sup>b</sup>	129.6 <sup>a</sup>
X ( <sup>1</sup> BR)	113.3 <sup>a</sup> ; 87.8 <sup>b</sup>	65.6 <sup>a</sup>
X ( <sup>3</sup> BR)	94 <sup>a</sup> ; 65.6 <sup>b</sup>	54.3 <sup>a</sup>
2	-39.3 <sup>a</sup> ; -79.4 <sup>b</sup>	-151.3 <sup>a</sup>

<sup>a</sup> From AM1. <sup>b</sup> From PM3.

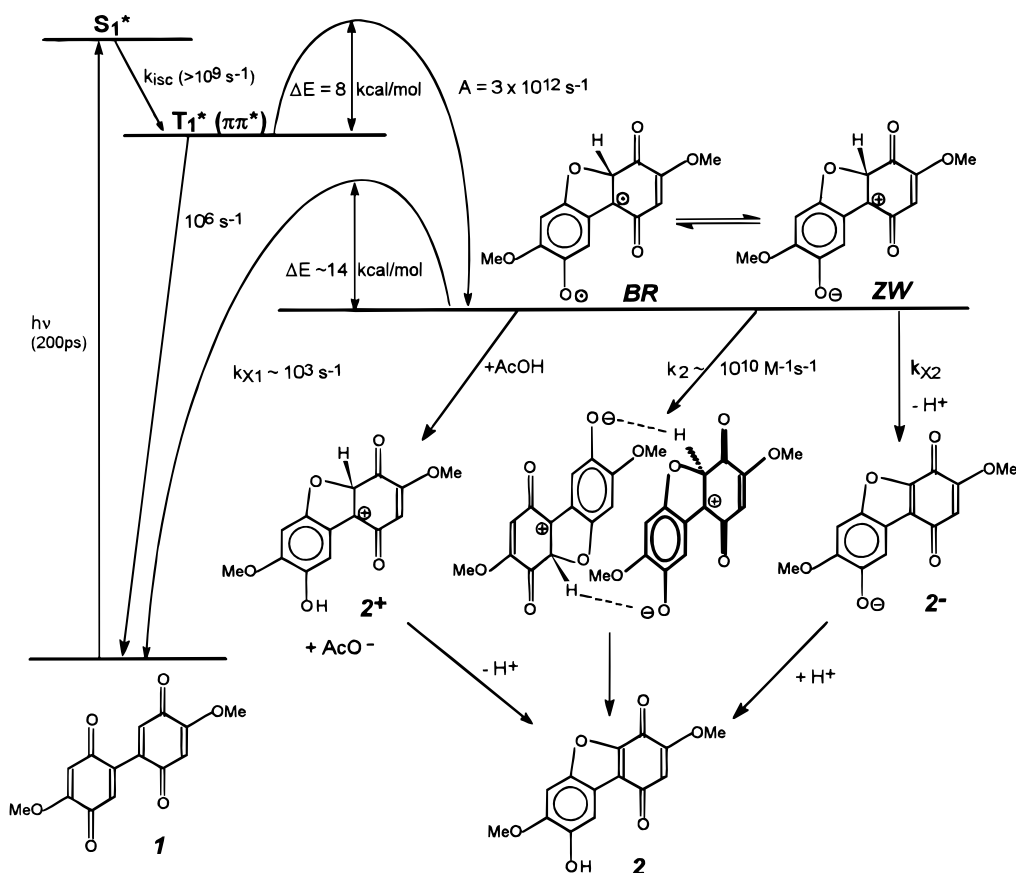
which can be drawn as a zwitterion or a biradical as shown in Scheme 3, are probably different.

**Structure of the X Intermediate.** As stated above, the X intermediate is most probably first produced as a triplet biradical, <sup>3</sup>BR, since the frequency factor  $A_1$  associated to  $k_{TX}$  clearly corresponds to a spin-allowed process but it may rapidly equilibrate with, or be transformed into, a singlet biradical, <sup>1</sup>BR, or a zwitterionic species, ZW. The BR structure includes a moiety which resembles a semiquinone radical known to absorb in the 410–420 nm range.<sup>27</sup> For instance X' does show an absorption band with a maximum at 440 nm.<sup>26</sup> That the absorption spectrum of X does not show any band in this region argues against a BR structure. The shift of the maximum of the absorption band of X in the red from 750 nm in acetonitrile to 800 nm in benzene indicates that the ground state of X is more stabilized by a polar solvent than the excited state involved in this optical transition. This may be rationalized by assuming ZW and BR structures for the ground and excited states of X, respectively.

On the other hand, the reactivity of X with AcOH is surprisingly low for a ZW structure including a phenolate moiety, whereas the large rate constant of the reaction of X' with AcOH is in agreement with a ZW structure for X'. Thus, spectroscopic considerations are in favor of a ZW structure for X and a BR one for X' but the reactivity with AcOH suggests the reverse.

Enthalpies of formation of the initial and final products, 1 and 2, and those of the ZW, <sup>1</sup>BR and <sup>3</sup>BR structures of X have been calculated using the AM1 and MP3 modules of AMPAC

## SCHEME 4: Reaction Mechanism as It Appears from This Study



6.01.<sup>28</sup> The relative  $\Delta H$  values, with **1** taken as reference, given by these calculations are listed in Table 7.

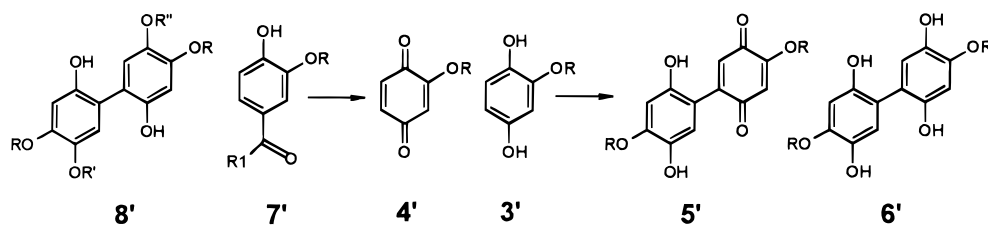
Considering the uncertainty on these values and the effect of solvation, these calculations do not allow to decide which is, from the ZW and BR structures, the lowest in energy. The ZW and <sup>1</sup>BR structures appear to be nearly isoenergetic (with the <sup>3</sup>BR being about 21 kJ/mol lower). By contrast, the same calculations performed on the **AnBQ** system give the BR structures to be 63 to 75 kJ/mol lower in energy than the ZW one. This strongly suggests that, in agreement with the above spectroscopic considerations, **X'** is a biradical and implies that the reactivity of the **X** and **X'** species with acetic acid does not give valid information about the structure of these species. As shown in Figure 5, the calculated distribution of electron density is nearly the same in ZW and <sup>1</sup>BR structures of **X**. Along the chain O(19)–C(3)–C(2)–C(1)–C(7), the small changes in the charge on the various atoms are not as expected from the mesomeric structures: the negative charge on O(19) is about the same in both cases, C(7) is not positively charged in ZW but is even more negative than in <sup>1</sup>BR, by 0.17  $e^-$  unit, and the most important other change affects C(2) by only 0.1  $e^-$  unit.

It thus appears that the ZW and <sup>1</sup>BR structures of **X** are nearly indistinguishable so that **X** would be a mixture of these two limit structures in equilibrium, through <sup>1</sup>BR, with <sup>3</sup>BR. The substantial difference between the absorption spectra of **X'** and **X** suggests that the latter would be mainly ZW: this seems possible when assuming that the difference in energy between <sup>1</sup>BR and <sup>3</sup>BR is overestimated by calculations and that solvation will favor a ZW structure.

**Special Mechanism under LFP Conditions.** Under laser flash photolysis conditions, in benzene as well as in acetonitrile, the decay of **X** is largely due to a second-order process with

$k_2/\epsilon \approx 1.7 \times 10^6 \text{ cm s}^{-1}$  in benzene at 840 nm and  $\approx 0.55 \times 10^6 \text{ cm s}^{-1}$  in acetonitrile at 750 nm. Values of  $\epsilon \approx 4000 \text{ M}^{-1}\text{cm}^{-1}$  in benzene at 840 nm and about  $8000 \text{ M}^{-1}\text{cm}^{-1}$  in acetonitrile at 750 nm were obtained by the relative actinometry technique using the absorption of the benzophenone triplet state as standard<sup>29</sup> and taking into account the values of  $\Phi_{\text{TX}}$ . This yields values of  $k_2$  around 6.4 and  $4.0 \times 10^9 \text{ M}^{-1} \text{ s}^{-1}$  in benzene and acetonitrile, respectively, close to the diffusion controlled limit. The transient absorbance measured in the 700–800 nm region being around 0.04 in benzene and 0.08 in acetonitrile, the maximum concentration of **X** is about 10  $\mu\text{M}$  in both solvents so that the value of  $k_2[\text{X}_{\text{max}}]/k_1$  is about 8 in benzene and 2 in acetonitrile. Numeric integration indicates that the yield of products resulting from the second-order process is then about 5 and 1.5 times larger than that the yield of products resulting from the first-order process. Therefore, especially in benzene, the final products obtained under our LFP conditions mainly result from the second-order decay of **X**. It has been noted above that, after the full decay of **X**, the amplitude of the final increase of the absorbance in the 400–550 nm region, assigned to **2**, is nearly the same in benzene as in acetonitrile. Clearly, the second-order process of decay of **X** produces the benzofuran **2** with a high efficiency, in benzene as well as in acetonitrile. The encounter of two **X** species in the head-to-tail position, as shown in Scheme 4, is favored since the zwitterionic structure most probably contributes largely to the real structure of the **X** species, and easily gives two benzofuran molecules by mutual exchange of the H atom located at the cyclization center. Consequently, the quantum yield of the reaction in benzene increases when the experimental conditions of irradiation favor the formation of high concentrations of **X** and, therefore, the encounter of two **X** species. Under irradiation with a frequency-

## SCHEME 5: Structures of Some Molecules of Interest



tripled Q switch Nd<sup>3+</sup> laser (BMI, 20 ns,  $\approx$  20 mJ/pulse, 1 Hz) of samples in a 10 mm cell with an absorbance at 355 nm,  $A_{355}$ ,  $\approx$  1.0, the ratio of the rates of formation of **2** in acetonitrile and benzene is around 2, whereas it is at least equal to 5 under continuous irradiation. The value of this ratio decreases to 1.4 when the laser beam is slightly focused with a cylindrical cell and irradiates the sample in a 2 mm cell with  $A_{355} \approx$  0.2 (i.e., in conditions which mimic those of LFP experiments).

Finally, if the encounter of two **X** species does not occur in the head-to-tail position, it may give a dimer-type product which could explain that the absorption spectrum obtained after irradiation under LFP conditions shows, in the 330–400 nm region, an absorption significantly larger than the absorption spectrum obtained after continuous irradiation.

## Conclusion

The mechanism of the photoconversion **1**  $\rightarrow$  **2**, as established by this study, is represented in Scheme 4. In all of the tested experimental conditions, the chemical yield is equal (or very close) to unity since the (main) reactions competing with the formation of **2** restore the initial compound **1**.

The overall quantum yield, which can reach (and probably exceed) 60 to 70% in deaerated and warm polar solvents, is only around 3% in aerated nonpolar solvents at room temperature. Its temperature dependence is explained by the large activation energies (around 33 and 58 kJ/mol, respectively) associated with two elementary reactions of this mechanism, one on the way to the final product, the other one restoring the initial compound.

Let us recall that **1** is a model compound for products which may be formed by photolysis and oxidation of lignin. These products would certainly differ from **1** by additional substitution(s) and/or by changes of the methoxy substituents to other alkoxy groups. Most probably, the values of the above-mentioned activation energies would be affected by these changes in the substitution pattern. From the "rule" relating  $\Delta G$  and  $\Delta E$  for a given reaction in an homogeneous series of compounds, any structural change inducing a relative stabilization of the **X** intermediate is expected to decrease  $\Delta E$  for the cyclization step  $^3\mathbf{1}^* \rightarrow \mathbf{X}$  and to increase  $\Delta E$  for the reopening step  $\mathbf{X} \rightarrow \mathbf{1}$ , both of these changes acting toward an increase of the quantum yield. Changes of the  $\Delta E$  values by 4 or 8 kJ/mol may increase or decrease the quantum yield by 1 or 2 orders of magnitude.<sup>30</sup>

The postulated structure of lignin does not include the bis-methoxyquinone moiety or even an hydroxy-alkoxybiphenyl structure such as **8'** which could be considered as an obvious precursor of the bis-alkoxyquinone. By contrast, it includes a number of alkoxy *p*-carbonyl phenols (**7'**) which may give rise to alkoxyhydroquinones (**3'**) and alkoxybenzoquinones (**4'**).

The reaction studied can be relevant for the process of yellowing of lignocellulosic materials only if it is preceded by a reaction of coupling of the substituted quinones/hydroquinones to give a bis-hydroquinone (**6'**) or the dihydro-bisquinone (**5'**) the (photo)oxidation of which will give the bis-quinone. This

coupling reaction is known in the case of the system hydroquinone/*p*-benzoquinone (unsubstituted) in slightly basic aqueous solution and its mechanism was studied by Boule et al.<sup>31</sup> On the other hand, photolysis of the quinone **4** in aerated dimethoxyethane gives probably the dimeric products **5** and/or **6** since dibenzofuran **2** was observed as one of the final products.<sup>11</sup> In the latter case, the irradiation was given in the quinone absorption band (Rayonet 350 UV lamps), whereas in the former it was given in the absorption band of the hydroquinone. The real mechanism of the coupling reaction(s) **4** + **4**  $\rightarrow$  **5** and/or **4** + **3**  $\rightarrow$  **6** still needs to be elucidated.

The effect of substituents on the values of the activation energies of the elementary reaction involved in the reaction bisquinone  $\rightarrow$  dibenzofuran and the mechanism of the coupling reaction yielding the bisquinone are currently under investigation.

**Supporting Information Available:** Some of the results of a study of the photocyclization of the *m*-anisylbenzoquinone (transient absorption spectra, quantum yield, and kinetic measurements as a function of the concentration of acetic acid and oxygen in the solvent) are given and interpreted to support the mechanism proposed for this reaction. This material is available free of charge via the Internet at <http://pubs.acs.org>.

## References and Notes

- Norström, H. *Svensk Papperstid.* **1969**, *72*, 32.
- Déglise, X.; Merlin, A. *L'actualité Chimique*, **1994**, *7* (suppl.), 156.
- Castellan, A. *L'actualité Chimique*, **1994**, *7* (suppl.), 148.
- Sharman, P. M. *Pulp Pap.* **1989**, *63*(5), S3–S32.
- Zhang, L.; Gellerstedt, G. *Acta Chem. Scand.* **1994**, *48*, 490–497.
- Argyropoulos, D. S.; Heitner, C.; Schmidt, J. A. *Res. Chem. Intermed.* **1995**, *9*, 263.
- Leary, G. *Nature* **1968**, *217*, 672.
- Anderson, E. L.; Pawlak, Z.; Owen, N. L.; Feist, W. C. *Appl. Spectrosc.* **1991**, *45*, 641.
- Lee, D. Y.; Sumimoto, M. *Holzforchung* **1991**, *45* (suppl.), 15.
- Hirashima, H.; Sumimoto, M. *Tappi J.* **1994**, *77* (1), 146.
- Forsskåhl, I.; Gustafsson, J.; Nybergh, A. *Acta Chem. Scand.* **1981**, *B35*, 389.
- Shand, A. J.; Thomson, R. H. *Tetrahedron* **1963**, *19*, 1919.
- Kuznets, V. M.; Levin, P. P.; Khudyakov, I. V.; Kuzmin, V. A. *Izv. Akad. Nauk. SSSR, Ser. Khim.* **1978**, 1284.
- Bruce, J. M.; Chaudry, A. U. H.; Dawes, K. *J. Chem. Soc., Perkin Trans. I* **1974**, 288.
- Akiba, M.; Kosugi, Y.; Okuyama, M.; Takada, T. *J. Org. Chem.* **1978**, *43*, 4472.
- Bonneau, R.; Moufid, H.; Guyot, G. *New J. Chem.* **1991**, *15*, 257.
- Marquardt, R.; Granjean, S.; Bonneau, R. *J. Photochem. Photobiol. A: Chem.* **1992**, *69*, 143.
- Erdtman H. G. H. *Proc. R. Soc. London (A)* **1933**, *143*, 191.
- Shand, A. J.; Thomson, R. H. *Tetrahedron* **1963**, *19*, 1919.
- Heller, H. G.; Langan, J. R. *J. Chem. Soc. Perkin Trans. II* **1981**, 341.
- Reichardt, C. *Angew. Chem., Int. Ed. Engl.* **1979**, *18*, 98.
- Reichardt, C. *Justus Liebigs Ann. Chem.* **1971**, *752*, 64. Dimroth, K.; Reichardt, C. *Justus Liebigs Ann. Chem.* **1969**, *727*, 93.
- Calculated with  $[O_2] = 7.8$  mM in EtOH, 9.1 mM in benzene (Murov, S. L. *Handbook of Photochemistry*; M. Dekker, Inc.: New York, 1973; p 89.) and 8.4 mM in MeCN (daSilva, A. M.; Formosinho, S. J.; Martins, C. T. *J. Chromatogr. Sci.* **1980**, *18*, 180) for O<sub>2</sub>-flushed solutions.

(24) These values depend strongly on the values  $k_0$ ,  $A$ , and  $\Delta E$  used for calculation of  $\Phi_{TX}$ . We used the values given in Table 4.

(25) The values of  $A_{X1}$  and  $A_{X2}$  should be multiplied by 2 (or 5) if  $\Delta E_{X2} = 1.7$  (or 4.2) kJ/mol.

(26) Letellier, M.; Hannachi, Y.; Bonneau, R. *See Supporting Information*.

(27) Bridge, N. K.; Porter, G. *Proc. R. Soc. (London) A* **1958**, 244, 259.

(28) The authors gratefully acknowledge the help of Dr. M. Kreissler in performing these calculations.

(29) Bonneau, R.; Carmichael, I.; Hug, G. L. *Pure Appl. Chem.* **1991**, 63, 289.

(30) Calculations indicate that the overall quantum yield in benzene at 27 °C,  $\approx 8\%$  with  $\Delta E$  values equal to 33.5 and 58.5 kJ/mol (this study) would be  $\approx 70\%$  with  $\Delta E$  values = 29.5 and 67 kJ/mol and  $\approx 0.1\%$  with 37.5 and 50 kJ/mol.

(31) Boule, P.; Rossi, A.; Pilichowski, J. F.; Grabner, G. *New J. Chem.* **1992**, 16, 1053.